Proton scattering from an excited nucleus ($^{18}F^m$, $J^\pi = 5^+$, $E_x = 1.1$ MeV) using a γ-ray-tagged secondary isomeric nuclear beam

J. A. Brown,* F. D. Becchetti, J. Jänecke, D. A. Roberts, D. W. Litzenberg, T. W. O'Donnell, and R. E. Warner†
Department of Physics, University of Michigan, Ann Arbor, Michigan 48109

N. A. Orr‡ and R. M. Ronningen
National Superconducting Cyclotron Laboratory, Michigan State University, East Lansing, Michigan 48824
(Received 14 February 1994; revised manuscript received 15 August 1994)

We have used γ-ray tagging to identify a secondary isomeric beam of the short-lived, high-spin isomer $^{18}F^m$ ($E_x = 1.1$ MeV, $J^\pi = 5^+$) produced at the K1200 cyclotron at the National Superconducting Cyclotron Laboratory. Elastic scattering of $p+^{18}F^m$ at $E_{c.m.} \approx 20$ MeV was observed using the characteristic γ decays of $^{18}F^m$ ($T_{1/2} = 163$ ns) to identify the state of the projectile *after* the scattering, thus minimizing the probability of excitation of the beam and, hence, nonelastic scattering.

PACS number(s): 25.60.+v, 25.40.Cm, 25.70.Bc, 27.20.+n

I. INTRODUCTION

Secondary beams of β-delayed γ emitters and isomeric radioactive nuclear beams (RNB's) present new possibilities in the study of heavy-ion reactions not available using stable beams [1–4]. The technique of γ-ray tagging is a powerful tool both in identifying radioactive nuclear beams and in observing reaction products which decay with the nearly prompt (e.g., less than a few ms) emission of characteristic γ rays. The flux, energy, and transmission of specific isomeric beams can be readily optimized even in a mixed secondary beam by observing the characteristic γ decay(s) of the isomer.

Highly deformed and "halo" nuclei, which are both typical of many RNB's, have been predicted to exhibit rather large enhancements in their nuclear reaction rates, viz., by a factor of 2–100 in the total nonelastic reaction cross sections including the total fusion and breakup cross sections [3–5]. Large-angle elastic scattering cross sections should then be significantly affected, since these are sensitive to the absorptive parts of the optical model scattering potential [6]. RNB's may have very large spins, i.e., larger than conventional stable nuclear beams, so that enhanced spin-spin and spin-orbit effects not previously observed might play a role in their scattering.

However, a common problem with the use of most secondary beams is the poor energy resolution of the beam which is typically a few percent, i.e., several MeV. This makes it difficult to separate purely elastic scattering from nonelastic scattering which involves excitation of either the projectile or the target. Especially at large scattering angles, the nonelastic and elastic scattering cross sections can be comparable [6]. This makes interpretation of the data dependent on theoretical calculations of the nonelastic reaction channels [7]. Other nuclear reactions involving RNB's which involve unresolved final states of either the projectile or the target are likewise more difficult to analyze.

In contrast, the use of γ-tagged beams, in particular certain isomeric beams, provides unique opportunities to study heavy-ion (HI) reactions which preserve the initial state of the projectile. These include both elastic scattering as well as nuclear reaction studies. Isomeric nuclei may play an important role in nucleosynthesis, and development of relatively pure, high-intensity isomeric beams provides a method to study relevant isomeric-beam-induced reactions in the laboratory [1–4].

Very high intensity, highly focused isomeric beams could, conceivably, provide a high density of nuclei with an inverted nuclear level population suitable as the first element of a γ-ray laser [1–3]. Also, the unique γ rays from isomeric beams and the wide choice of isomer half-lives make these beams potentially useful for imaging implanted ions in atomic and biological media [3].

Some studies of reactions involving radioactive targets enriched with long-lived metastable isotopes, in particular $^{178}Hf^{m2}$ ($J^\pi = 16^+, T_{\frac{1}{2}} = 31$ yr), have been reported or are in progress. These include both nuclear-physics and atomic-physics experiments [8–10]. However, in many of these experiments the isotopic mixture in the target presents a considerable background problem and hence the data obtained, particularly for nuclear-physics studies, have been limited. Much better control of both the isotopic purity and the isomeric purity of the isomer nucleus can be obtained if, instead, one can produce a secondary isomeric beam. Nuclear reactions in particular can then be studied in an inverse kinematics mode

*Present address: National Superconducting Cyclotron Laboratory (NSCL), Michigan State University, East Lansing, MI 48824.
†On leave from Department of Physics, Oberlin College, Oberlin, OH 44074.
‡Present address: LPC-ISMRA, Boulevard du Marechal Juin, 14050 Caen Cedex, France.

with a heavy-mass beam on a light-mass target and, in addition, the γ decay of the isomer can often be utilized to identify and tag the isomer beam. This was done in the present experiment where we produced and then scattered a high-flux, high-purity, secondary isomeric beam $^{18}F^m$.

The isomer $^{18}F^m$ ($J^\pi = 5^+$) is a very high spin projectile (Fig. 1); in particular, its spin is higher than any β-stable heavy-ion beam with $A \leq 30$. Thus, as noted above, one might expect enhanced spin-orbit and spin-spin effects in the scattering potentials described by the nuclear optical model potential. We have measured the elastic scattering of $^{18}F^m + p$ at $E_{c.m.} \approx 20$ MeV by detecting the recoil proton, the recoil $^{18}F^m$, and the coincident $^{18}F^m$ γ rays. This allowed us to measure the center-of-mass (c.m.) scattering angle reasonably well ($\pm$ 4°) despite the small ($\leq$ 3° laboratory) deflection of the scattered $^{18}F^m$. The isomer γ-tagging technique, utilizing a large HPGe γ detector in coincidence with recoil particles, was used to separate the scattering of protons and $^{18}F^m$ from that of $^{18}F_{g.s.}$ where the latter may be mixed with the beam or produced by the scattering itself.

II. EXPERIMENTAL SETUP

Secondary beams of the short-lived, excited, isomeric nucleus $^{18}F^m$ (J^π=5$^+$, E_x = 1.1 MeV, $T_{1/2}$ = 163 ns) have been produced with the K1200 cyclotron at the National Superconducting Cyclotron Laboratory (NSCL) at Michigan State University using the single-nucleon transfer reaction $^{12}C(^{17}O,^{18}F^m)^{11}B$ at a primary ^{17}O beam energy of 30 MeV/nucleon [11–13]. Recently, high yields of isomers in secondary beams produced from fragmentation or other reactions have also been reported [14–17]. We use the single-nucleon "direct transfer" method [11] because single-nucleon transfer reactions such as (^{12}C,^{11}B) typically have sufficiently high cross sections ($\geq$ 10 mb/sr) to make secondary beams ($> 10^3$/s) usable in nuclear reaction studies. In addition, these reactions preferentially populate high-spin "stretched" single-particle states arising from $(j_1 \otimes j_2)_J$ with $J = J_{max} \equiv |j_1 + j_2|$ where the latter often form an isomeric state (Fig. 1) and typically are low in excitation [18]. Since the neutron and proton orbits in $^{18}F^m$ are coplanar with the neutron and proton coupled to form an $S = 1$ "deuteron" (Fig. 2), one can describe $^{18}F^m$ as a "deuteron" orbiting a $J^\pi = 0^+$ ^{16}O core with ℓ_d=4$\hbar$, with a moderately strong binding energy of the "deuteron" to the ^{16}O core (6.4 MeV). The high angular momentum associated with the valence "deuteron" in $^{18}F^m$ is predicted [13] to substantially increase (viz., by $\sim$ 40%) the radial extent of $^{18}F^m$ (Fig. 2) relative to $^{18}F_{g.s.}$, $^{18}O_{g.s.}$, or $^{16}O_{g.s.}$ since the latter are low-spin nuclei ($J^\pi = 1^+, 0^+$, and 0^+, respectively).

Among the many isomeric RNB's feasible [12,13] we selected the isomer $^{18}F^m$ for this experiment since its half-life is long enough (163 ns) to transport the beam to a secondary target, yet short enough to use fast particle-γ coincidence techniques to identify the subsequent isomer gamma decays. High-energy $^{18}F^m$ beams at the NSCL have been developed and utilized in experiments using the University of Michigan's 7 T superconducting solenoid system installed there [19]. The latter system has a large collection efficiency and the short flight path ($\sim$ 3 m) minimizes the $^{18}F^m$ decays in flight. Therefore it can produce a beam with $>$ 70% of the ^{18}F secondary beam in its isomeric state ($^{18}F^m$) with an intensity $> 10^4$/s. Unfortunately, the high neutron flux associated with the 0° alignment of the solenoid and its short flight path limited the use of hyperpure germanium γ-ray detectors (HPGe) at the secondary target position since HPGe is susceptible to neutron damage. Therefore, except for related $^{18}F^m$ beam development, the measurements reported here were done with a secondary $^{18}F^m$ beam produced using the A1200 superconducting magnet system at the NSCL [20]. This magnet system uses dipole beam-bending magnets well separated from the secondary target chamber by a thick shielding wall and provides a much reduced fast neutron background at the focal point of the secondary $^{18}F^m$ beam [13].

The flight path of the $^{18}F^m$ from the A1200 production target was minimized by using only the second half of the

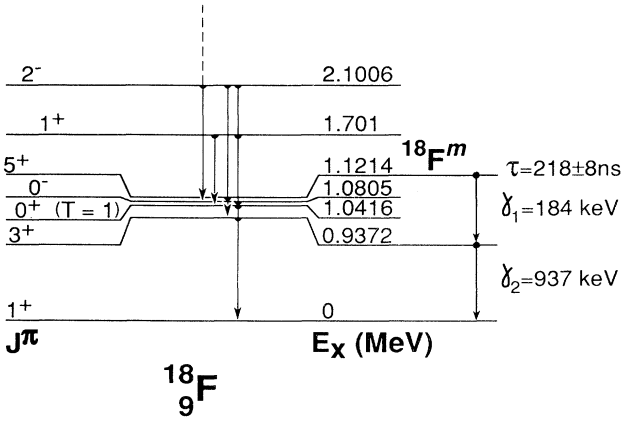

FIG. 1. Level scheme for ^{18}F showing the low-lying levels and γ decays. The mean lifetime for the $^{18}F^m$ level is indicated along with its γ decays (see also Figs. 4 and 6). Except as noted the levels have total isospin $T = 0$. The data are adopted from those given by F. Ajzenberg-Selove, Nucl. Phys. **A392**, 1 (1983).

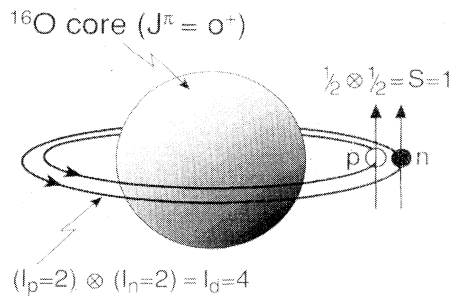

FIG. 2. A schematic diagram of the structure of the $J^\pi = 5^+(1d_{\frac{5}{2}})^2$ isomeric state in ^{18}F, E_x=1.12 MeV (see Fig. 1).

A1200 magnet system with the production target placed at the position normally used as the intermediate focal plane of the A1200 system [20]. Nonetheless, the flight path was sufficiently long ($\sim$ 8 m) to allow appreciable decay of the $^{18}F^m$ in flight (but mostly inside the well-shielded A1200 vault). This, combined with the reduced collection efficiency associated with the use of a dipole magnet rather than a solenoid, resulted in a focused $^{18}F^m$ beam of intensity of about 10^3/s, with an isotopic purity, i.e., the ratio of ^{18}F and $^{18}F^m$ relative to other ions, of about 50%, with 50%–60% of the ^{18}F ions in turn being in the $J^\pi = 5^+$, $^{18}F^m$ isomeric state. This secondary beam was then used to study p+$^{18}F^m$ elastic scattering ($E_{c.m.} \approx 20$ MeV) in reverse kinematics. Subsequent measurements of $^{18}F^m$ + Si total reaction cross sections [21] using the UM 7 T solenoid will be reported elsewhere [22].

The experimental setup is shown in Fig. 3. The HPGe detector was placed in an aluminum reentrant vacuum flange, typically <10 cm from the ΔE-E silicon detector telescope used to identify the ^{18}F ions. The HPGe γ detector had an intrinsic efficiency of about 30% relative to a 7.6 cm $\times$ 7.6 cm NaI detector for ^{60}Co γ rays ($E_\gamma \doteq 1.3$ MeV). The overall detection efficiency of the HPGe in the geometry used was determined to a few percent using a calibrated mixed γ-ray source. Initially the ΔE-E silicon detector HI telescope, which consisted of a 600 mm^2, 414 μm Si ΔE detector backed by a 600 mm^2, 418 μm Si E detector, was positioned at $\theta = 0°$ (Fig. 3). The A1200 magnets were suitably tuned to produce the maximum amount of $^{18}F^m$ as determined by the ^{18}F yield in the ΔE-E counter telescope and the $^{18}F^m$ γ rays detected in the HPGe. Thus, the production, intensity, and both the isotopic and isomeric purity of the secondary isomeric beam could be monitored using the unique $^{18}F^m$ γ-decay lines $5^+ \rightarrow 3^+$ (184 keV) and $3^+ \rightarrow 1^+$ (937 keV) to identify the beam and optimize its yield. Typical γ-ray spectra obtained to optimize production of $^{18}F^m$ are shown in Fig. 4.

The HPGe γ detector also provides an accurate, continuous monitoring of the yield of $^{18}F^m$ from the $^{12}C(^{17}O, ^{18}F)^{11}B$ production reaction. As an example, it was possible to easily detect even slight changes in the beam tuning conditions, including small shifts in the primary ^{17}O beam energy and hence the secondary $^{18}F^m$ beam energy, since the ratio of $^{18}F^m$ to all ^{18}F, i.e., the isomer purity, changed significantly (see Fig. 4). Normally such changes are difficult to detect in secondary-beam experiments [3,4]. As a consequence, we generally obtained much better long-term energy resolution using $^{18}F^m$ monitored with γ rays than typically is obtained with other secondary beams [13].

An energy profile of the $^{18}F^m$ beam which has been stopped at $\theta = 0°$ in the silicon detector HI particle telescope (Fig. 3) and which is in coincidence with $^{18}F^m$ γ rays in the HPGe γ-ray detector (Fig. 4) is shown in Fig. 5 (see also below). As noted, this capability of optimizing and subsequently "tagging" the isomeric beam by its characteristic γ decays allows one to perform experiments in difficult mixed-beam situations. Hence, this technique could also be extended to include γ decays of β-decaying nuclei of sufficiently short half-lives.

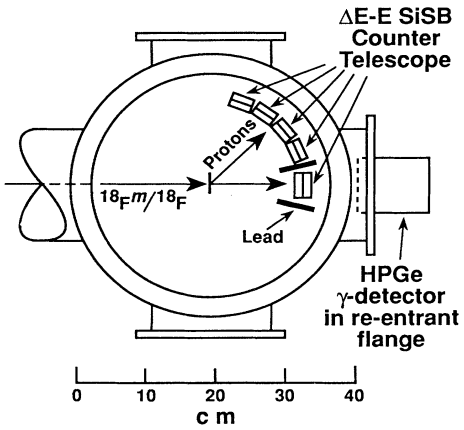

FIG. 3. Experimental setup used to measure the elastic scattering of $^{18}F^m$ from a 4 mg/cm^2 CH_2 target. The scattered $^{18}F^m$, the recoil proton, and the subsequent $^{18}F^m$ decay γ rays can all be detected in coincidence.

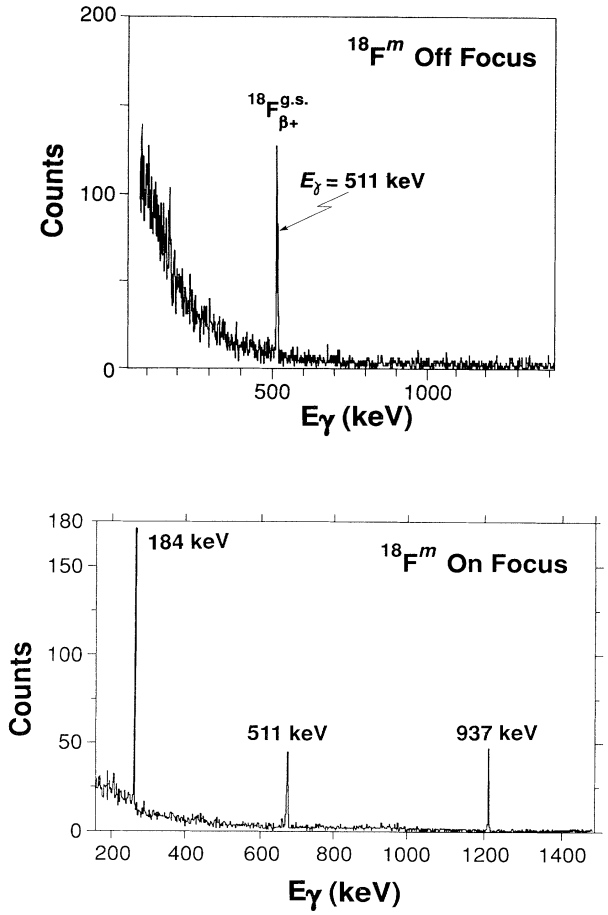

FIG. 4. HPGe γ-ray spectra obtained at $\theta = 0°$ (Fig. 3) for a $^{18}F \doteq {}^{18}F_{g.s.}$ beam (top) and an optimized $^{18}F^m$ beam (bottom).

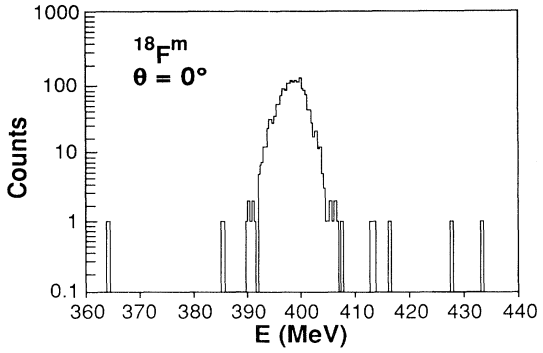

FIG. 5. A γ-tagged $^{18}F^m$ beam-energy profile observed at $\theta = 0°$ (Fig. 3).

III. MEASUREMENTS

In another $^{18}F^m$ experiment where we measured total reaction cross sections [22], the $^{18}F^m$ beam was typically reduced to an intensity of about 10^2/s so that individual beam particles and the corresponding individual reaction products could be identified event by event and, where appropriate, the individual $^{18}F^m$ beam particles tagged by their subsequent γ decays. However, in the scattering of $^{18}F^m$, as reported here, we used the maximum possible beam ($\geq 10^3$/s). We then forgo identifying individual incoming beam particles since the use of the direct transfer method [11–13] to produce the beam and the subsequent monitoring of the isomeric purity using the unique isomer γ rays (Fig. 4) ensure that the ^{18}F beam of interest is primarily $^{18}F^m$ or a known mixture of $^{18}F_{g.s.}$ and $^{18}F^m$.

Thus, we first observed the recoiling $^{18}F_{g.s.}$, $^{18}F^m$, or other heavy ions stopped and identified in the HI ΔE-E telescope as being in fast coincidence with a recoil proton or other light ion's (LI's) identified in one of the LI ΔE-E counter telescopes (Fig. 6). We then recorded the γ-ray energy and time spectra from the HPGe γ-ray detector in fast coincidence (typically $\Delta t < 1$ μs) with both the HI and LI particle detectors. The latter, together with the accurate ΔE-E information, served to identify the recoiling HI as either $^{18}F^m$, $^{18}F_{g.s.}$, or as another heavy ion.

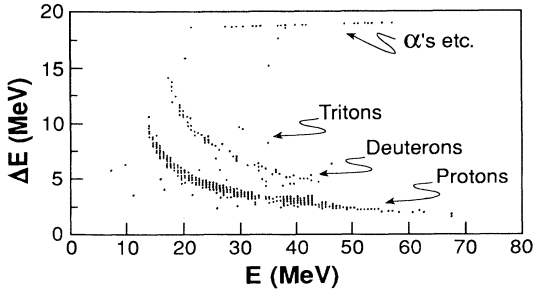

FIG. 6. A ΔE-E particle identification spectrum (ungated) in the most forward angle light-ion counter telescope, $\theta = 30°$. The ions shown are in coincidence with any heavy-ion recoil (Fig. 3) and not necessarily just $^{18}F^m$.

The possibility that the isomeric state can be populated by inelastic scattering of the g.s. component of ^{18}F in the beam at the secondary target or in the stopping detector is an important consideration when using this γ-tagging technique. Fortunately, since it involves proton-induced inelastic excitation of a high-spin isomeric level (Fig. 1) this probability is calculated to be small (a few percent or less) relative to the proton elastic scattering and the LI transfer reaction channels.

The spectrum of γ rays observed in coincidence with heavy ions in the forward counter telescope (Fig. 3) and a recoil ion in the light-ion counter telescope is shown in Fig. 7. Typical ΔE-E spectra of the corresponding light ions (Fig. 6) observed in coincidence with γ-tagged $^{18}F^m$ recoil ions are shown in Fig. 8. As expected for a CH_2 target (Fig. 3), almost all of the light ions in coincidence with forward-recoiling $^{18}F^m$ ions are recoil protons from elastic scattering [13]. The kinematic coincidence between the HI and LI reaction products would also allow one to generate an energy-loss or "Q-value" spectrum which could cancel out part of the large energy spread [$\sim$ 15 MeV full width at half maximum (FWHM) here] in the incident secondary beam [23], which is important for certain reaction channels (see below). This would be independent of the detection of a $^{18}F^m$ γ ray.

While double- and triple-coincident events (Figs. 6–8) are clearly identified, viz., HI-LI and HI-LI-$^{18}F^m$ γ-ray coincidences, respectively, with the HPGe γ detector available and its location outside the scattering chamber, even in a reentrant thin aluminum window [13] the required threefold coincidence greatly limits our statistics in the present arrangement. Thus, we could detect only one γ ray for about every 50 proton -^{18}F coincidences. Since the ^{18}F beam was typically $\geq$ 50% $^{18}F^m$ and the overall isomeric fraction was monitored by the $^{18}F^m$ γ rays (Fig. 4), some information on scattering of the excited beam was obtained with better statistics ($\times$50 more events) without the full triple-coincidence requirement. In fact, for this type of measurement which only uses the isomeric γ rays to monitor the beam purity, a somewhat longer-lived, high-purity isomeric beam would be adequate provided one could resolve inelastic excitation.

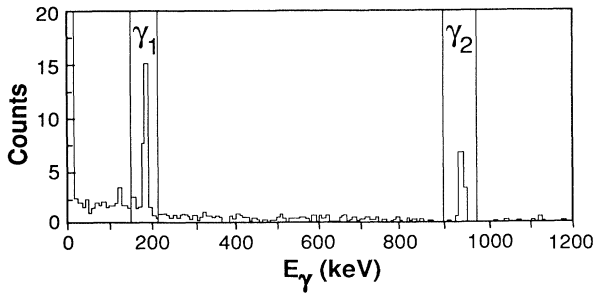

FIG. 7. Energy spectrum of γ rays observed in coincidence with ^{18}F and $^{18}F^m$ in the forward counter telescope and a recoil ion in any one of the light-ion counter telescopes (Fig. 3). The two lines (Fig. 1) from the decay $^{18}F^m \rightarrow {}^{18}F_{g.s.}$ are indicated.

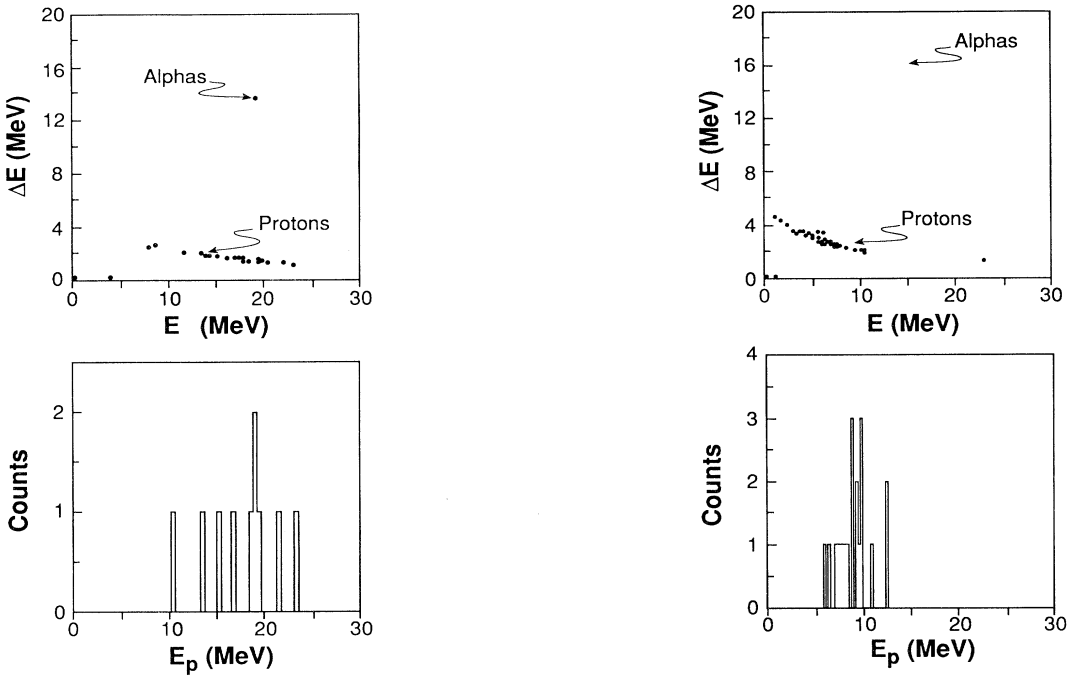

FIG. 8. Light-ion ΔE-E and gated, projected proton recoil energy spectra detected in coincidence (Fig. 7) with γ-tagged $^{18}F^m$ ions as observed in various ΔE-E detectors shown in Fig. 3 [$\theta_p = 60°$ (left) to 67.5° (right)].

We display, in Fig. 9, the elastic scattering from protons of the mixed $^{18}F_{g.s.}+^{18}F^m$ beam (approximately a 50%-50% mixture) as a ratio to Rutherford scattering, σ/σ_R, where we do not require the fast coincident $^{18}F^m$ γ rays from the stopped, recoiling $^{18}F_{g.s.}$ or $^{18}F^m$ ion in the HI telescope (Fig. 3). Although the data shown oscillate well above Rutherford scattering at large angles, the absolute cross section at those angles is quite small (a few mb/sr) since the Rutherford scattering cross section itself falls off rapidly with angle [as $\sin^{-4}(\theta_{c.m.}/2)$]. As observed in other cases of proton scattering, any anomalous scattering due to specific partial-wave resonances or potential-scattering effects can cause significant deviations ($\times 5$ or more) in the σ/σ_R values at large scattering angles [6,7,24–26]. As can be seen in Fig. 9, the deviations from Rutherford scattering, σ_R, are comparable to those observed for $^{16}O+p$,$^{18}O+p$, and $^{20}Ne+p$ at $E_{c.m.} \doteq$ 20 MeV [26].

The dampening of the oscillations observed in σ/σ_R (Fig. 9) is characteristic of scattering from stable deformed nuclei or nuclei with low-lying excitation modes [26–28]. However it must be noted that the data shown, like many of the reported "elastic" scattering measurements of high-energy RNB's [3,4], can include unresolved inelastic scattering since the energy resolution of the secondary beam is usually poor, e.g., $\geq$10 MeV (Fig. 4). This is not sufficient to resolve inelastic excitations of the ^{18}F (Fig. 1) although with protons (as here) this is calculated to be small relative to the elastic scattering where $\sigma \gg \sigma_R$. (This is *not* the case for HI-HI scattering where typically $\sigma \ll \sigma_R$ [6].) Therefore we deduce that the 50%–60% $^{18}F^m$ component in the scattered $(^{18}F_{g.s.}+^{18}F^m)+p$ probably has no significant anomalous scattering (i.e., $\sigma/\sigma_R \geq 50$) at large angles ($\theta_{c.m.} > 60°$).

Likewise the ratio of γ-tagged $^{18}F^m + p$ elastic scattering to non-γ-tagged $(^{18}F^m + {}^{18}F_{g.s.})+p$ scattering, where again the latter is approximately a 50%-50% mixture, can be used to set some limits. These data are shown in Fig. 10 together with the ratio expected based on the measured HPGe γ-tagging efficiency. Except for slight increases near $\theta_{c.m.} = 60°$ and perhaps $\theta_{c.m.} = 110°$, there appear to be no systematic, large (e.g., $> \times 5$) differences between $^{18}F^m+p$ and $^{18}F_{g.s.}+p$ scattering. This appears

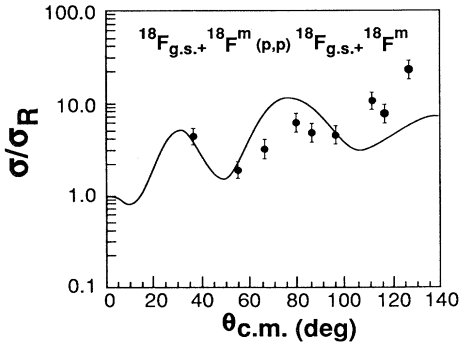

FIG. 9. The elastic scattering of the $(^{18}F_{g.s.}+^{18}F^m)$ mixed beam (50% each) from protons at $E_{c.m.}$=20 MeV. The curve is an OM calculation based on $^{18}O+p$ and $^{20}Ne+p$ parameters determined near the same c.m. energy [26].

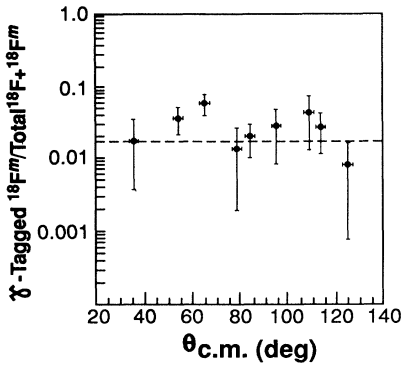

FIG. 10. Ratio of elastic scattering cross sections observed for γ-tagged $^{18}F^m + p$ relative to a mixture (approximately 50% each) of $^{18}F_{g.s.} + ^{18}F^m$. The dashed curve is the ratio expected based on the HPGe γ efficiency (Fig. 3) assuming the same elastic scattering for $^{18}F_{g.s.} + p$ and $^{18}F^m + p$ (see text).

to be true even at large scattering angles where one might again expect increased sensitivity due to absorptive and spin effects in the elastic scattering potentials due to the unusual, unique structure of $^{18}F^m$ (Fig. 2).

The elastic scattering angular distribution for $^{18}F^m(E_x = 1.1$ MeV, $J^\pi = 5^+) +$ proton obtained with the full triple-coincidence requirement (^{18}F recoil ion + recoil proton + isomeric γ decay) is shown in Fig. 11. In Fig. 11 (top) we also compare our results with an optical model (OM) calculation based on the $^{18}O+p$ and $^{20}Ne+p$ parameters of Fabricci *et al.* [26] which were measured at c.m. energies between 17.7 and 44.1 MeV. (Since due to slight uncertainties in the absolute fluxes of the secondary beams the most accurate way to monitor the integrated secondary beam flux was the forward-angle elastic scattering, which is closest to Rutherford scattering, we have normalized the forward-angle $^{18}F^m + p$ scattering to the OM calculations.) A better OM fit is obtained (Fig. 11, bottom) when V_{SO} is increased, as discussed below.

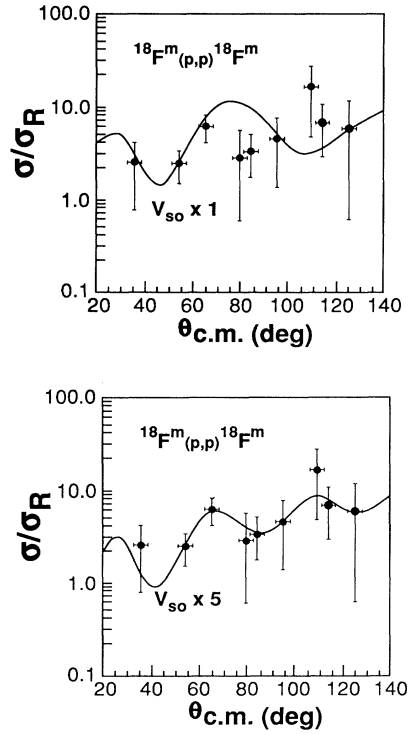

FIG. 11. Top: Elastic scattering angular distribution of γ-tagged $^{18}F^m + p$, $E_{c.m.} \doteq 20$ MeV as ratio to Rutherford scattering. The filled circles are the experimental points and the curve is an optical model calculation based on $^{18}O+p$ and $^{20}Ne+p$ OM parameters (see Ref. [26]). Bottom: Same as above, but with the spin-orbit strength (V_{SO}) increased by $\times 5$.

IV. ANALYSIS AND DISCUSSION OF RESULTS

While the present $^{18}F^m+p$ results are limited by statistical uncertainties from the low γ-tagging efficiency, they are consistent with predictions using conventional optical model parameters for this mass and energy region [26]. They show no large-scale anomalous effects. As an example, if we adjust the absorptive part of the optical model potential to produce a large increase ($\geq \times 2$) in the total nonelastic reaction cross section, similar to some predictions [5] and recent measurements at low energies [22], we find σ/σ_R could approach 100 at large angles. This is excluded at the 1σ level by the present, if limited, $^{18}F^m + p$ data (Fig. 11) and, in addition, by the $^{18}F_{g.s.}+^{18}F^m$ data (Fig. 9).

This is especially true if we use the integrated cross section data which are more accurate. A comparison of the calculated nuclear reaction cross sections indicates that any anomalous effects contribute, at most, about 20% to the total nuclear reaction cross section, viz., ≤ 300 mb out of 1400 mb. Thus, we do not appear to observe any unusual $p+^{18}F^m$ scattering at $E_{c.m.} = 20$ MeV as might be expected [22] on the basis of anomalous absorption (i.e., enhanced nuclear reactions) involving the $^{18}F^m$ (Fig. 2).

The present data can serve to place some limits on the magnitude of the spin-orbit and spin-spin terms in the OM for high spins, although in general these effects [25–28] are much less pronounced than those noted above for absorptive effects. Unfortunately due to the very high spins involved ($5^+ \otimes \frac{1}{2}^+$), most commonly available elastic scattering optical model codes cannot properly calculate the appropriate spin-orbit and spin-spin couplings [25].

Nonetheless we have estimated the effect of the unusual, high-spin ($J^\pi = 5^+$) isomeric configuration of $^{18}F^m$ as a target by allowing the OM code to search for both the spin-orbit coupling strength and the absorptive part of the OM potential. The parameter V_{SO} can approximately simulate spin-orbit and spin-spin effects on the elastic scattering cross section while the absorption parameters (W_S and W_D) can account [7] for an enhancement [22] in nuclear reaction cross sections due to the extended configuration of $^{18}F^m$ with its valence "deuteron" (Fig. 2) and the possible breakup $^{18}F^m \rightarrow d+^{16}O$.

We find that a surprisingly good quantitative fit is obtained (Fig. 11, bottom) by allowing V_{SO} to increase to

$\times 5$ relative to its normal value [26]. In contrast, adjusting the absorptive potential $W(r)$ alone did not produce such an improvement. This indicates that any differences between $^{18}F^m + p$ and $^{18}F_{g.s.} + p$ (or $^{18}O+p$) elastic scattering can most likely be attributed to spin-dependent effects. This is consistent with the spin-dependent effects (a few percent) observed [27] in the scattering of polarized neutrons from polarized ^{27}Al ($J^\pi = \frac{5}{2}^+$), even if one scales by $\times 2$ or so for the increased spin of $^{18}F^m$. It has also been noted that large static deformations (as expected for $^{18}F^m$; see Fig. 2) can generate *effective* spin-dependent interactions without the necessity of introducing nuclear spin-spin interactions. The impact on the elastic scattering is expected to be modest, though, which is consistent with the present results [28].

V. LIMITS ON "SUPERELASTIC" ($Q > 0$) SCATTERING

A more intense $^{18}F^m$ beam and increased γ-tagging efficiency should allow one to search for "superelastic" scattering, i.e., inelastic scattering of $^{18}F^m$ with $Q > 0$ such as Coulomb deexcitation. Such scattering has been reported for atomic collisions involving metastable atoms [29,30] as well as low-energy neutron scattering from a mixed $^{178}Hf/^{178}Hf^{m2}$ target [8] although the latter experiment, as noted, had significant background problems. The present data (see, e.g., Fig. 8) although limited in statistics, can set some limits on this process. It is found that the "superelastic" scattering $^{18}F^m + p \rightarrow ^{18}F + p$ ($Q = +1.1$ MeV) is $< 50\%$ of the $p+^{18}F^m$ elastic scattering at $\theta_{c.m.} = 20°$–$140°$. As noted earlier this is not necessarily a trivial result since at large angles elastic and inelastic scattering, including superelastic scattering, can be comparable [6].

VI. CONCLUSIONS

The present studies indicate that prompt γ tagging is a powerful technique for identifying short-lived isomeric nuclear beams and selecting light-ion and heavy-ion reaction channels where the initial beam state is preserved during the reaction. Since high-purity secondary isomeric nuclear beams (including perhaps highly deformed shape isomers) appear to be preferentially made by transfer reactions [11–13,16] and certain fragmentation reactions [14,15,17], this should permit study of a variety of unusual and perhaps new types of nuclear reactions at present and future RNB facilities.

As an example, recently [22] we have used the high-purity $^{18}F^m$ secondary beam developed with the UM 7 T solenoid installed at the NSCL to make measurements of the total nonelastic reaction cross section [21] of $^{18}F_{g.s.}$ +Si and $^{18}F^m$ +Si. These measurements, which exhibit some unusual features, will be described in detail elsewhere [22]. We are similarly pursuing other experiments which will utilize the high spin of $^{18}F^m$ and other isomer beams [12,13] to provide unique angular momentum selection rules (and other features) in specific types of nuclear reactions.

ACKNOWLEDGMENTS

The authors thank J. Kolata, K. Lamkin, J. Bajema, A. Nadasen, B. Sherrill, and the staff at NSCL for their assistance. This work was supported in part by the National Science Foundation under Contracts Nos. PHY-9208468, PHY-9122067, PHY-8913815, and PHY-9214992. The University of Michigan 7 T solenoid was funded under DOE Contract No. DE-FG02-88ER75445 (University Instrumentation Program).

[1] *Proceedings of the Accelerated Radioactive Beams Workshop*, Parksville, Canada, 1985, edited by L. Buchmann and J. M. D'Auria (TRIUMF, Vancouver, 1985).
[2] *Proceedings of the First International Conference on Radioactive Nuclear Beams*, Berkeley, California, 1989, edited by W. D. Myers, J. M. Nitschke, and E. B. Norman (World Scientific, Singapore, 1990).
[3] *Proceedings of the Second International Conference on Radioactive Nuclear Beams*, Louvain-la-Neuve, Belgium, 1991, edited by Th. Delbar (Institute of Physics and Physical Society, Bristol, England, 1991).
[4] *Proceedings of the Third International Conference on Radioactive Nuclear Beams*, East Lansing, Michigan, 1993, edited by D. J. Morrissey (Editions Frontières, Gif-sur-Yvette, France, 1993).
[5] N. Takigawa, H. Sagawa, and T. Shinozuka, Nucl. Phys. **A538**, 221c (1992).
[6] A. Nadasen *et al.*, Phys. Rev. C **37**, 132 (1988).
[7] M. S. Hussein and G. R. Satchler, Nucl. Phys. **A567**, 165 (1994).
[8] I. A. Kondurov, E. M. Korotkikh, Yu. V. Petrov, and G. I. Shuljak, Phys. Lett. **106B**, 383 (1981).
[9] Th. Happ *et al.*, GSI Scientific Report 1992, 1993, p. 91; H. J. Wollersheim, in *Future Directions in Nuclear Physics with* 4π *Gamma Detection Systems of the New Generation*, edited by J. Dudek and B. Haas, AIP Conf. Proc. No. 259 (AIP, New York, 1992).
[10] G. Rotbard *et al.*, Phys. Rev. C **48**, R2148 (1993).
[11] F. D. Becchetti *et al.*, Phys. Rev. C **42**, R801 (1990).
[12] F. D. Becchetti *et al.*, Nucl. Instrum. Methods Phys. Res. B **56/57**, 554 (1991).
[13] J. A. Brown *et al.*, in [3], p. 45; J. A. Brown *et al.*, in [4], p. 317; J. A. Brown, Ph.D. thesis, University of Michigan, 1993.
[14] B. M. Young *et al.*, in [4]; p. 437.
[15] B. M. Young *et al.*, Phys. Lett. B **311**, 22 (1993).
[16] V. Borrel, in [4], p. 135; J. L. Uzureau *et al.*, Phys. Lett. B **331**, 280 (1994).
[17] K. Matsuta *et al.*, in [4], p. 377.
[18] E. Rivet, R. Pehl, J. Cerny, and B. G. Harvey, Phys. Rev. **141**, 1021 (1966).
[19] F. D. Becchetti *et al.*, Nucl. Instrum. Methods Phys. Res. B **79**, 326 (1993).
[20] B. M. Sherrill *et al.*, in [2], p. 72; Nucl. Instrum. Methods

B **56/57**, 1106 (1991).
[21] R. E. Warner *et al.*, Phys. Rev. C **48**, 245 (1993).
[22] D. Roberts *et al.*, in *Proceedings of International Symposium on Physics of Unstable Nuclei*, Nigata, Japan, 1994 [Nucl. Phys. A (in press)].
[23] N. R. Fletcher, Nucl. Instrum. Methods Phys. Res. A **316**, 143 (1992).
[24] J. M. Blatt and V. F. Weisskopff, *Theoretical Nuclear Physics* (Dover, New York, 1991); P. E. Hodgson, *Nuclear Reactions and Nuclear Structure* (Clarendon Press, Oxford, 1991), Chaps. 5–10.
[25] A. P. Stamp, Phys. Rev. **153**, 1052 (1967); A. Lindner, Nucl. Phys. **A155**, 145 (1970).
[26] E. Fabricci *et al.*, Phys. Rev. C **21**, 830 (1980); J. L. Escudié *et al.*, *ibid.* **10**, 1645 (1974).
[27] C. R. Gould *et al.*, Phys. Rev. Lett. **57**, 2371 (1986).
[28] V. Hnizdo and K. W. Kemper, Phys. Rev. Lett. **59**, 1892 (1987); Phys. Rev. C **38**, 1242 (1988).
[29] G. D. Latyscheff and A. I. Leipunsky, Z. Phys. **65**, 111 (1930).
[30] S. N. Foner and R. L. Hudson, J. Chem. Phys. **25**, 601 (1956); **37**, 1662 (1962).

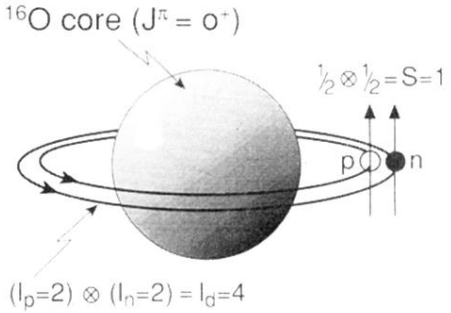

FIG. 2. A schematic diagram of the structure of the $J^{\pi} = 5^{+}(1d_{\frac{5}{2}})^2$ isomeric state in ^{18}F, E_x=1.12 MeV (see Fig. 1).